Modeling of Impact Phenomena with Biped Locomotion Mechanisms – Theory and Experiments

Aleksandar Rodić, PhD (Eng)[1]
Prof. Khalid Addi, PhD (Eng)[2]
Prof. Georges Dalleau, PhD (Eng)[3]

This paper suggests a generalized approach to the mathematical modeling of biped locomotion systems (humans or humanoid robots) with a special attention paid to impact and contact dynamics. Modeling of impact dynamics with different locomotion mechanisms has a significant importance in robotics and military applications due to the necessity of mechanism adaptation to unknown and unstructured terrains. Instead of the usual *inductive* approach that starts from the analysis of different situations of real motion (walking, running, jumping, climbing the obstacles, taking up the loads, etc.) and tries to make a generalization, a *deductive* approach is pursued, whereby an entirely general problem is considered. Impact dynamics is modeled applying the Linear Complementarity Problem (LCP) formulation. General methodology is explained and demonstrated with humanoid robots via the synthesis of a spatial biped model. The validity of the modeling approach is proved by experimental measurements on a human subject in laboratory conditions. Plenty of graphic presentations illustrating experimental results as well as the results of the corresponding simulations tests are shown.

Key words: robotics, locomotion systems, system modeling, mathematical modeling, contact dynamics, contact load, impact load.

Introduction

CURRENTLY many researchers in biomechanics and robotics are dealing with different problems of locomotion of humans and humanoid robots [1]-[4]. The analysis of the foot-ground contact is essential in biomechanics to investigate its consequences on the human body. Humanoids, being the future of robotic science, are becoming more and more human-like in all aspects of their functioning. It is expected that they will replace humans in a variety of tasks. Thus, it is generally accepted that their shape and motion should be based on bio-mechanical principles. Broad research results from biomechanics and humanoid robotics are applied to military purposes building special robotized systems to assist soldiers or to replace human power by artificial robotic systems. In that sense, the US army (the Defense Advanced Research Projects Agency (DARPA)) has initialized a project entitled "Super Soldier" [5]. Drugs, genetic enhancements and technology would allow for regeneration, faster healing, muscle strength enhancement up to current olympic levels, endurance of an Alaskan sled dog, cognitive enhancement, operating without sleep for many days without performance degradation, the metabolic energy of a twenty-year old for a forty or fifty-year old and immunity to pain. Soldiers equipped with high-tech gear that make them stronger, swifter and smarter - invulnerable to bullets and able to survive the harshest conditions. Some of the ideas being explored include battle suits embedded with tiny devices that can seal against chemical attack, administer immediate medical care and even - no joke, scientists say - give soldiers the power to leap over small buildings. The Sarcos exoskeleton [5] (Fig.1) just needs a good powersource and engine to power the hydraulics for it to enhance the strength and endurance of someone who wears it by ten times. It should be possible for someone with the untethered Sarcos exoskeleton to carry and use heavy weapons. The person wearing the exoskeleton can carry 100-200kg without being tired.

Because of the complexity and high requirements imposed on such robots, their control system has to utilize the accurate dynamic models. So, the control, the design, and the simulation, strongly require general dynamic models that will make humanoid robots and walking mechanisms capable of handling the increasing diversity of expected tasks [6, 7].

The paper is concerned with a generalized approach [6] to the modeling of biped systems. It explains the principles, derives the general methodology and proves the validity of the approach through comparison with the experimental results. Special attention is paid to the modeling of the unilateral impact/contact phenomena during a conventional biped locomotion. With human beings, a function of the footwear is supposed to attenuate the impact forces and the transient vibrations. To investigate this function, several models were proposed in the literature by assuming only single impact point or by assigning some viscous elastic properties to the shoe sole [8, 9]. It was also underlined that

[1] Institute of Mihajlo Pupin, Volgina 15, 11060 Belgrade, SERBIA
[2] Université de la Réunion, LIM, 97490 Saint-Denis, FRANCE
[3] Université de la Réunion, CURAPS-DIMPS, 97430 Le Tampon, FRANCE

the mechanical properties of the footwear can altered the gait patterns due to their influence to the sensory feedback [10]. Sensory feedback from the feet may affect specific motor unit pools during different activities [11]. The modeling of the interface between the foot and the ground is then important to understand the role of foot impact on the gait control or on the tissue damage. However, the existing contact models do not take into account the multi-point contacts of the feet with the ground. In that sense, a valid model of the impact/contact dynamics is tried to be identified taking into account both the biped dynamics and the environment dynamics will be considered in the paper. The problem of modeling the impact dynamics is solved by implementing the mathematical methodology known in the literature as the Linear Complementarity Problem formulation (LCP) [12, 13]. The authors are well aware of the extreme complexity of the problem of modeling biological systems [6, 14], which stems from the complexity of the mechanical structure and actuation. The fact that the control of a biological system is a still insufficiently studied area contributes greatly to the significance of the problem. Because of that the authors start with the dynamic modeling of the structure of biped mechanisms, which yields a solid approximation of dynamics of the mechanical aspect of human motion.

Figure 1. Sarcos exoskeleton [5] designed to multiply man power in military tasks

Modeling of a biped locomotion mechanism

In this paper, a biped locomotion mechanism of the anthropomorphic structure will be considered as a mechanical representative of the human body. In a mechanical sense, a biped mechanism represents a multi-body, large-scale dynamic system with a variable structure. Thus the entire mechanism, keeping its lump mass constant, changes its inertial properties due to the motion of biped links at the joints of the arms, legs and trunk. Besides, due to the motion of the mechanism as well as due to the influence of the external disturbances acting upon the system or carrying the payload the contact forces and contact moments arise at the particular points of the biped mechanism. In this paper, only the contacts of the biped mechanism with environment at its end points (the foot is assumed to be rectangular) are considered [15, 16]. This, however, does not lower the generality of the considered principles of modeling of a biped mechanism.

Let the joints of the system be such to allow n independent motions. Let these joint motions be described by joint angles forming the vector of the generalized coordinates $q = [q_1 \cdots q_n]^T$. The terms 'joint coordinates' or 'internal coordinates' are commonly used for this vector in robotics. This set of coordinates describes completely the relative motion of the links. With the basic link (e.g. pelvis) in the chain fixed, the system would have n DOFs. However, the basic link in the chain is not fixed but allowed to perform six independent motions in space. Let the position of the basic link be defined by the three Cartesian coordinates (x, y, z) of its mass center and the three orientation angles (φ-roll, θ-pitch and ψ-yaw), forming the vector $\underline{X} = [x\ y\ z\ \varphi\ \theta\ \psi]^T$. Now, the overall number of DOFs for the system is $N = 6 + n$, and the system position is defined by

$$Q = [\underline{X}\ q]^T = [x\ y\ z\ \varphi\ \theta\ \psi\ q_1 \cdots q_n]^T \qquad (1)$$

It is assumed that each joint has an appropriate actuator. This means that each motion q_j has its own drive – the torque τ_j. Note that there is no drive associated to the basic body coordinates $\underline{X}$. The vector of the joint drives is $\tau = [\tau_1 \cdots \tau_n]^T$, and the augmented drive vector (N-dimensional) is $T = [\underline{0}_6\ \tau]^T = [0 \cdots 0\ \tau_1 \cdots \tau_n]^T$. Similarly, with human beings muscles represent biological power-trains. Pairs of muscles by their synchronized contractions and extensions move the bones of the skeleton at its joints.

The dynamic model of the biped mechanism (humanoid) has the general form [6, 14]:

$$H(Q,d)\ddot{Q} + h(Q,\dot{Q},d) = \tau + J^T(Q,d)\,F$$
$$h(Q,\dot{Q},d) = h_{ccf}(Q,\dot{Q},d) + h_g(Q,d) \qquad (2)$$

or decoupled

$$H_{\underline{X},\underline{X}}\ \ddot{\underline{X}} + H_{\underline{X},q}\ \ddot{q} + h_{\underline{X}} = \underline{0}_6 + J_{\underline{X}}^T\ F$$
$$H_{q,\underline{X}}\ \ddot{\underline{X}} + H_{q,q}\ \ddot{q} + h_q = \tau + J_q^T\ F \qquad (3)$$

The dimensions of the inertial matrix and its submatrices are: $H(N \times N)$, $H_{\underline{X},\underline{X}}(6 \times 6)$, $H_{\underline{X},q}(6 \times n)$, $H_{q,\underline{X}}(n \times 6)$, and $H_{q,q}(n \times n)$. The dimensions of the vectors containing centrifugal, Coriolis and gravity effects are: $h(N)$, $h_{\underline{X}}(6)$, and $h_q(n)$. The vector $h(Q,d)$ consists of two vectors: the vector of centrifugal and Coriolis' forces $h_{ccf}(Q,\dot{Q},d)$ and the vector of gravity forces and moments $h_g(Q,d)$. Dimension of the vector of ground reaction, external load

and disturbance forces is $F(m \times 1)$. The dimensions of the Jacobi matrix and its submatrices are $J(m \times N)$, $J_X(m \times 6)$, $J_q(m \times n)$. The vector $d(l)$ represents a parameter vector including geometry (link lengths, positions of the link mass centers), as well as the corresponding dynamic parameters (link masses, moments of inertia) of the robotic system.

Modeling of Foot Contact Dynamics

Let us consider the link of the biped mechanism that has to establish contact with some external object. In the case considered, it is the foot tha moves towards the ground, strikes it and stays in contact (e.g. walking, running or climbing the stairs). An external object may be immobile (like ground), or mobile, like part of some other dynamic system (mobile platform [17, 18], conveyer, boat, tram, tank, etc.). To express mathematically the forthcoming contact, the motion of the considered link should be described by an appropriate set of coordinates. Since the link is a body moving in the 3D-space, it is necessary to consider six coordinates. Let this set be $\underline{g} = [g_1, \cdots, g_6]^T$ and let call them functional coordinates (Fig.2a). Functional coordinates are introduced [6] as relative ones, defining the position of the link with respect to the ground (object) to be contacted. A consequence of the rigid link-object contact is that the link and the object perform some motions, along some axes, jointly (Fig.2b). These are constrained (restricted) directions (e.g. g_3, g_5, Fig.2b). Let there be m such directions. A relative position along these axes does not change. Along the other axes (e.g. g_1, g_2, g_4, g_6, Fig.2b) a relative displacement is possible. These are unconstrained (free) directions. In order to get a simple mathematical description of the contact, $\underline{g}$-coordinates are introduced to describe the relative position. The zero value of a coordinate indicates the contact along the corresponding axis.

So, the motion of the external object (to be contacted) has to be known (or calculated from the appropriate mathematical model), and then the $\underline{g}$-frame fixed to the object (the plane π in this case, Fig.2) is introduced to describe the relative position of the link in the most proper way. Thus, in a general case, the $\underline{g}$-frame is mobile. As the link is approaching the object, some of $\underline{g}$-coordinates reduce and finally reach zero. The zero value means that the contact is established. These functional coordinates (which reduce to zero) are called restricted coordinates and they form the subvector $\underline{g}^c$ of the dimension m. The other functional coordinates are free and they form the subvector $\underline{g}^f$ of the dimension $6 - m$. Now, one can write:

$$[\underline{g}^c, \ \underline{g}^f]^T = K \cdot \underline{g} \tag{4}$$

where K is a 6×6 matrix used to rearrange the functional coordinates (elements of the vector $\underline{g}$) and bring the restricted ones to the first positions. In order to arrive at a general algorithm, the foot motion has to be described in a general way and, once the expected contact is specified, relate this general interpretation to the appropriate $\underline{s}$-frame.

The general description of the link motion assumes three Cartesian coordinates of a selected point of the link plus three orientation angles: $\underline{s}_l = [x_l \ y_l \ z_l \ \varphi_l \ \theta_l \ \psi_l]^T$, the subscript l standing for "link". These are absolute external coordinates in the *Oxzy* reference coordinate system (Fig.2a).

a)

b)
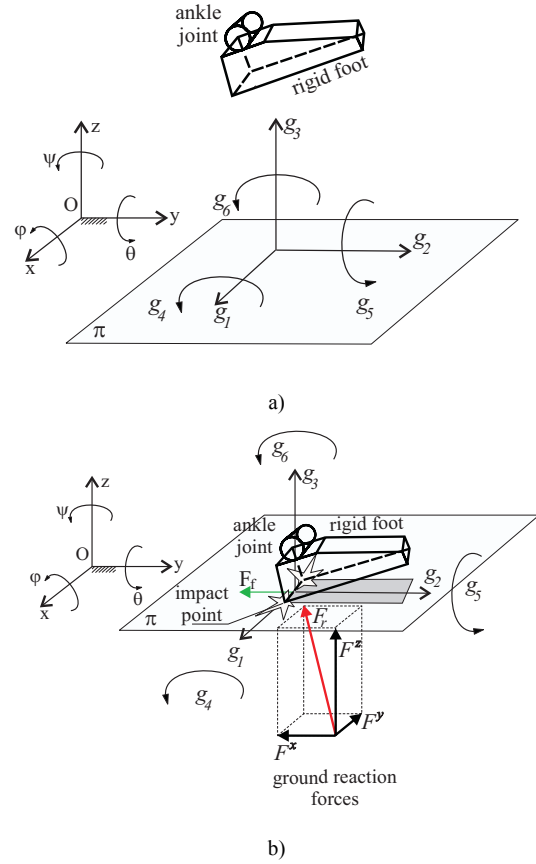
Figure 2. a) Functional coordinates of the foot contact; b) Rigid frictional impact along the foot edge

The relation between the link coordinates $\underline{s}_l$ and the system position vector Q defined in (1) is given by:

$$\underline{s}_l = \underline{s}_l(Q, d) \tag{5}$$

$$\underline{\dot{s}}_l = J_l(Q, d)\dot{Q} \tag{6}$$

$$\underline{\ddot{s}}_l = J_l(Q, d)\ddot{Q} + A_l(Q, \dot{Q}, d) \tag{7}$$

where

$$J_l = \frac{\partial \underline{s}_l}{\partial Q}$$

is a $6 \times N$ Jacobian matrix and

$$A_l = \frac{\partial^2 \underline{s}_l}{\partial Q^2} \dot{Q}^2$$

is a 6-dimensional adjoint vector. Let us concentrate on the object, i.e. the ground (example of an immobile object). In a general case, the object is mobile, so, its position is described by the absolute external coordinates:

$$\underline{s}_b = [x_b \ y_b \ z_b \ \varphi_b \ \theta_b \ \psi_b]^T,$$

the subscript b standing for "object".

When the $\underline{g}$-frame is introduced to define the relative position of the link with respect to the object, the coordinates will depend on both $\underline{s}_b$ and $\underline{s}_l$:

$$\underline{g} = \underline{g}(\underline{s}_l, \underline{s}_b) \tag{8}$$

or in the Jacobian form:

$$\underline{\dot{g}} = J_{gl}\,\underline{\dot{s}}_l + J_{gb}\,\underline{\dot{s}}_b \tag{9}$$

$$\underline{\ddot{g}} = J_{gl}\,\underline{\ddot{s}}_l + J_{gb}\,\underline{\ddot{s}}_b + A_g. \tag{10}$$

where the dimension of the Jacobi matrices is $J_{gl}, J_{gb} \in \Re^{6\times 6}$, and the dimension of the adjoint vector $A_g \in \Re^{6\times 1}$. Model (10) can be rewritten if the separation (4) and (7) is introduced. The model becomes:

$$\underline{\ddot{g}}^c = J_{gl}^c J_l \ddot{Q} + J_{gl}^c A_l + J_{gb}^c \underline{\ddot{s}}_b + A_g^c = \\ = J_{g,TOT}^c(Q,t)\ddot{Q} + A_{g,TOT}^c(Q,\dot{Q},t) \tag{11}$$

$$\underline{\ddot{g}}^f = J_{gl}^f J_l \ddot{Q} + J_{gl}^f A_l + J_{gb}^f \underline{\ddot{s}}_b + A_g^f = \\ = J_{g,TOT}^f(Q,t)\ddot{Q} + A_{g,TOT}^f(Q,\dot{Q},t) \tag{12}$$

where the model matrices are: $J_{g,TOT}^c = J_{gl}^c J_l$, $A_{g,TOT}^c = J_{gl}^c A_l + J_{gb}^c \underline{\ddot{s}}_b + A_g^c$, $J_{g,TOT}^f = J_{gl}^f J_l$ and $A_{g,TOT}^f = J_{gl}^f A_l + J_{gb}^f \underline{\ddot{s}}_b + A_g^f$.

Now, we are going to elaborate one representative type of contact with a special emphasis on the impact phase.

Modeling of Foot Impact

One may recognize the three phases of contact tasks [6, 7]:
(i)   approaching,
(ii) impact, and
(iii) regular contact motion.

The first phase is approaching. The link moves towards the object. All functional coordinates $\underline{g}$ are free but some of them (the subvector $\underline{g}^c$) reduce to zero.

The second phase is the impact. In the preceding phase (approaching), the motion of the link was planned so as to reach the object with a relative velocity equal to zero (collision-free contact). This is the reference motion. However, the control system produces the actual motion different from the reference. The tracking error leads to collision, a non-zero-velocity contact. The impact forces will affect the system state – after the impact the link state will comply with the object state and the type of contact.

The third phase is the regular contact motion. The contact forces make the link move according to the character of the contact.

In contact problems, the dynamic model has to take care of contact forces. Model (2), derived for a free biped, should be supplemented by contact forces. A contact force acts along each of constrained axis. So, there is a reaction force (or torque) for each coordinate from the set $\underline{g}^c$. There are m independent reactions. Let $F_r = [F_1, \cdots, F_m]^T$ be the reaction vector. If a coordinate g_j^c is linear (translational),

then the corresponding reaction F_j is a force. For a revolute coordinate, the corresponding reaction is a torque.

The contact-dynamics model is obtained by introducing reactions into the biped model (2):

$$H(Q)\ddot{Q} + h(Q,\dot{Q}) = \tau + J_{g,TOT}^c(Q,t)^T F_r \tag{13}$$

Since this model involves N scalar equations and $N + m$ scalar unknowns (vectors $\ddot{Q}$ and F_r), it is necessary to supply some additional conditions. The additional condition is the constraint relation adapted from (11) for $\underline{g}^c(t) = \underline{0} \Rightarrow \underline{\ddot{g}}^c(t) = \underline{0}$, containing m scalar equations. Now, relation (11) is replaced with

$$J_{g,TOT}^c(Q,t)\ddot{Q} + A_{g,TOT}^c(Q,\dot{Q},t) = \underline{0} \tag{14}$$

Then (13) and (14) describe the dynamics of a constrained biped, allowing one to calculate the acceleration vector $\ddot{Q}$ and the reaction vector F_r (thus enabling the integration and calculation of the system motion).

The impact phase starts when the biped link reaches the surrounding object(s). Strictly speaking, the restricted coordinates (elements of $\underline{g}^c$) reach zero one by one. So, a complex contact is established as a series of simpler contact effects. According to [6] the impact model is derived assuming that all the coordinates $\underline{g}^c$ attain zero simultaneously and establish a complex contact instantaneously. Let t_c' be the instant when the contact is established (restricted coordinates reduce to zero and the impact comes into action) and let t_c'' be the instant when the impact ends. So, the impact lasts for $\Delta t = t_c'' - t_c'$. For this analysis we assume that the impact is infinitely short, i.e. $\Delta t \to 0$. We also assume that the m coordinates (forming $\underline{g}^c$) reduce to zero simultaneously. We now integrate the dynamic model (13) over the short impact interval Δt:

$$H\Delta\dot{Q} = (J_{g,TOT}^c)^T F_r \Delta t \tag{15}$$

where

$$\Delta\dot{Q} = \dot{Q}(t_c'') - \dot{Q}(t_c') = \dot{Q}'' - \dot{Q}'. \tag{16}$$

During the approaching phase, the system model is integrated and the motion $Q(t), \dot{Q}(t)$ is calculated. Thus, the state at the instant t_c', i.e. $Q' = Q(t_c'), \dot{Q}' = \dot{Q}(t_c')$, is considered known. Since the object motion is also known, it is possible to calculate the model matrices $H, J_{g,TOT}^c$ in equation (15). The position does not change during $\Delta t \to 0$, and hence: $Q'' = Q(t_c'') = Q'$. Now, the model (15) (along with (16)), contains N scalar equations with $N + m$ scalar unknowns: the velocity after the impact, $\dot{Q}'' = \dot{Q}(t_c'')$ (dimension N), and the impact momentum $F_r \Delta t$ (dimension m). The additional equations needed to allow a solution are obtained starting from the constraint relation (14). Integrating (14) over $\Delta t \to 0$, one obtains

$$J_{g,TOT}^c(Q,t)\,\Delta\,\dot{Q} = 0\,. \tag{17}$$

i.e. the additional m scalar conditions. The augmented set of equations (15) and (17) (along with (16)) allow to solve the impact. The velocity after the impact, $\dot{Q}'' = \dot{Q}(t_c'')$, is found starting from the known state in t_c'. The impact momentum $F_r\,\Delta t$ is determined as well. The new state Q'', $\dot{Q}''$ represents the initial condition for the third phase, i.e. the regular contact motion.

Another approach, which is more realistic than an idealized single-point contact considered previously, deals with a multi-point frictional contact of the biped's feet. In this case, the restricted coordinates (elements of $\underline{g}^c$) reach zero one by one. The impact begins when the biped foot (feet) reaches the constraint surface π as presented in Fig.3. A constraint in a general case can be an ordinary curve, prismatic or flat surface. In the impact phase, the restricted coordinates $\underline{g}^c$ defined in (4) become zero. The existence of impact can be defined by the following conditions:

$$\underline{g}^c(t) = \underline{0},\ \underline{\dot{g}}^c(t) \le \underline{0} \tag{18}$$

In a general case, a foot impact to the constraint surface can be realized at an infinite number of points. Consequently, the problem would be numerically too complex. Because of that, a realistic approximation of the impact phenomenon has to be assumed. Without losing generality, four impact points (per foot contour $i = 1,\dots,4$ or $i = 5,\dots,8$, see Fig.3) instead of an infinite number of them can be assumed. Here, two contact points at the heel (i.e. $i = 1,2$ and $i = 5,6$, Fig.3) and two points at the front part of the foot (i.e. $i = 3,4$ and $i = 7,8$) will be considered. Generally, three possible unilateral impacts are possible: (i) single-point impact, (ii) two-points impact along the ordinary foot edge (e.g. the points i=5,6, Fig.3), and (iii) four-points impact (the case of a planar impact of the flat foot sole to the support). By considering the impact phenomenon as a series of simpler, unilateral contacts at the particular points one can perform a realistic analysis of the non-smooth, frictional biped contact dynamics.

Having in mind the above, some general assumptions should be put forward before deriving the non-smooth, multi-point impact model:

(i) The duration of the impact is "very short" $\Delta t(i) \to 0$.

(ii) Of the impact bodies can be generally divided in two phases: the compression phase and the expansion phase. Since the foot impact is followed by the compression phase, after which the biped foot stays completely or partly lying (pressed by biped weight) on the constraint surface, the expansion phase appears only in the special cases and will not be considered. The end of the compression phase is the start of the regular contact.

(iii) While the impact takes place (in the time interval Δt) the values of all the quantities of the multi-body system (biped mechanism) characterizing its position and orientation, as well as all non-impulse forces and torques (gravity, centrifugal and Coriolis'), remain constant.

(iv) Wave effects (elastic modes in the system) are not taken into account.

In the multiple-contact tasks such as a biped gait, for example, there may occur only one impact at one of the potential contact points or several impacts at several contacts simultaneously. The theory presented in the paper covers both possibilities. Here we will consider a system with $n_G = 8$ possible contact points. For this purpose four sets of indices are introduced to describe the kinematic state of each of the contacts.

Let then:

$$
\begin{aligned}
\Omega_G &= \{1, 2, \dots, n_G\} \\
\Omega_S &= \left\{i \in \Omega_G \mid g_N^{(i)} = 0\right\} \quad \text{with } n_S \text{ elements} \\
\Omega_N &= \left\{i \in \Omega_S \mid \dot{g}_N^{(i)} = 0\right\} \quad \text{with } n_N \text{ elements} \\
\Omega_{H1} &= \left\{i \in \Omega_N \mid \dot{g}_{Tl}^{(i)} = 0\right\} \quad \text{with } n_{H1} \text{ elements} \\
\Omega_{H2} &= \left\{i \in \Omega_N \mid \dot{g}_{Tt}^{(i)} = 0\right\} \quad \text{with } n_{H2} \text{ elements}
\end{aligned}
\tag{19}
$$

The locations of the impacts are given by the positions of the n_G contact points of Ω_G. Ω_S contains n_S indices of the constraints with a vanishing distance but arbitrary relative velocities, Ω_N describes the constraints which fulfil the necessary conditions for a continuous contact (vanishing distance and zero relative velocity in the normal direction), and Ω_{H1}, Ω_{H2} are those which are possibly sticking in two tangential directions – longitudinal and transversal. Numbers of elements of the sets $\Omega_S, \Omega_N, \Omega_{H1}, \Omega_{H2}$ are not constant because the contact configuration of the biped mechanism changes with time due to the stick-slip transitions, impacts and contact loss.
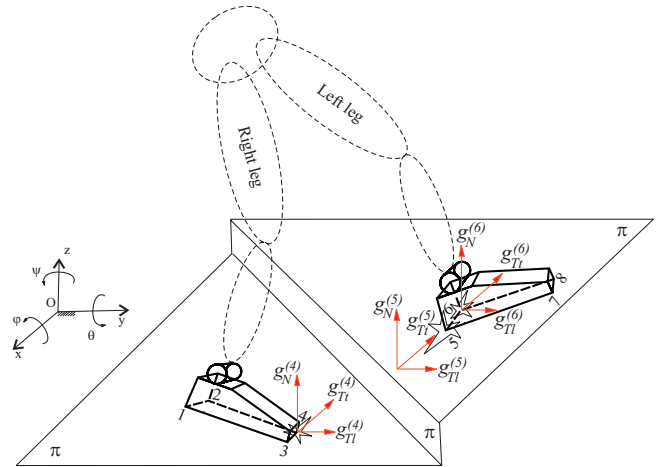
Figure 3. Multi-point contact of the biped links with the constraint surface π - the normal $g_N^{(i)}$ and the tangential directions $g_{Tl}^{(i)}, g_{Tt}^{(i)}$ of motion of the particular points $i = 1, \dots, 8$

For each contact point from Ω_G it is possible to determine the distance $g_N^{(i)}(Q,t)$ along the normal direction to the constraint surface. If one of these indicators becomes zero at the time instant $t'_c(i)$ and the corresponding relative velocity $\dot{g}_N^{(i)}$ is smaller than or equal to zero, an impact occurs. The contact is then closed and the unilateral constraint is active. The set od constraints which participate in the impact is then given by

$$\Omega_S^* = \left\{i \in \Omega_G \mid g_N^{(i)} = 0;\ \dot{g}_N^{(i)} \le 0\right\} \text{ with } n_S^* \text{ elements} \tag{20}$$

The set Ω_S^* contains all the sliding and sticking continuous-contact constraints $\left(g_N^{(i)}=0\right)$, as well as the impact contacts $\left(\dot{g}_N^{(i)} \le 0\right)$. This enables examining whether a contact separates under the influence of an impact at a different location i.

In order to determine the multi-point impact model, let us introduce the following functional coordinates $\underline{g}^{(i)}$, $i \in \Omega_S^*$ (see Fig.3). Instead of using the unified $\underline{g}$ (6×1)-vector of the functional coordinates (defined by (4)), the set of n_S^* (3×1)-vectors of the functional coordinates $\underline{g}^{(i)}$, $i \in \Omega_S^*$ will be introduced. In such a way, the relative positions of the biped feet are determined in the $\underline{g}^{(i)}$-frames, as shown in Fig.3. The functional coordinates $\underline{g}^{(i)}$ represent relative positions of the feet points i with respect to the corresponding frame attached to the constraint surface. In that sense, the normal $g_N^{(i)}$ and the tangential directions $g_{Tl}^{(i)}$ and $g_{Tt}^{(i)}$ are important. Tangential motions of the feet points are possible along the longitudinal $g_{Tl}^{(i)}$ as well along the transversal $g_{Tt}^{(i)}$ coordinate axes (Fig.3). The i-th vector of the functional coordinates $\underline{g}^{(i)}$, $i \in \Omega_S^*$ can be written in the form:

$$\underline{g}^{(i)} = \left[g_{Tl}^{(i)}, g_{Tt}^{(i)}, g_N^{(i)} \right]^T, i \in \Omega_S^* \qquad (21)$$

Bearing in mind the vector form (21), three components of impact forces can be defined in the same directions. They are: the normal impact force F_{N_i} in the $g_N^{(i)}$-direction of the restricted motion and the tangential impact forces F_{Tl_i}, F_{Tt_i} in the longitudinal $g_{Tl}^{(i)}$- and transversal $g_{Tt}^{(i)}$-directions. In a physical sense, the considered tangential forces represent the corresponding stiction or friction (sliding) forces acting in the plane that represents a constraint. The (3×1) vector F_{C_i} of the impact force acts at the i-th contact point C_i, $i \in \Omega_S^*$ and can be defined in the form:

$$F_{C_i} = \left[F_{Tl_i}, F_{Tt_i}, F_{N_i} \right]^T, i \in \Omega_S^* \qquad (22)$$

The positions of the contact points $C_i, i \in \Omega_S^*$ are always in the constraint area (or belong to the object that represents a constraint), and they are determined in the inertial coordinate system $Oxyz$. Let now $t_c'(i)$ be the instant when the i-th contact point of the foot and the constraint is established (i.e. when the restricted coordinate in the normal direction $g_N^{(i)}$ reduce to zero $g_N^{(i)}=0$ and the impact comes into action $\|F_{C_i}\|>0$) and let $t_c''(i)$ be the instant when the impact of the i-th point ends. So, the impact lasts for the time period $\Delta t(i) = t_c''(i) - t_c'(i)$.

When the $\underline{g}^{(i)}$-frame (defined by (21)) is introduced to determine the relative position of the i-th contour point at the foot with respect to the position of the contact C_i (lying in the constraint plane π, Fig.3), the coordinates $\underline{g}^{(i)}$ depend on both external coordinates $\underline{s}_{C_i}$ and $\underline{s}_{\pi_i}$:

$$\underline{g}^{(i)} = \underline{g}^{(i)}(\underline{s}_{C_i}, \underline{s}_{\pi_i}), \quad i \in \Omega_S^* \qquad (23)$$

$\underline{s}_{C_i}(Q,t) = \left[s_{C_i}^x, s_{C_i}^y, s_{C_i}^z \right]^T$ and $\underline{s}_{\pi_i}(t) = \left[s_{\pi_i}^x, s_{\pi_i}^y, s_{\pi_i}^z \right]^T$ are (3×1)-vectors that define position of the contact C_i of the biped foot as well as position of the corresponding point of the constraint surface π to be reached during the impact. The positions $\underline{s}_{C_i}$ and $\underline{s}_{\pi_i}$ are determined with respect to the inertial coordinate system $Oxyz$ (Fig.3). Then, a Jacobian form can be written as:

$$\underline{\dot{g}}^{(i)} = \left[\dot{g}_{Tl}^{(i)}, \dot{g}_{Tt}^{(i)}, \dot{g}_N^{(i)} \right]^T = J_{gC_i} \underline{\dot{s}}_{Ci} + J_{g\pi_i} \underline{\dot{s}}_{\pi_i}, \; i \in \Omega_S^* \quad (24)$$

Equation (24) can be projected onto the $\underline{g}^{(i)}$-frame axes $g_N^{(i)}, g_{Tl}^{(i)}, g_{Tt}^{(i)}$ (Fig.4). For this purpose three 3×1 unit vectors $\tilde{n}_i, \tilde{t}_{l_i}, \tilde{t}_{t_i}$ (collinear with the corresponding axes $g_N^{(i)}$, $g_{Tl}^{(i)}$, $g_{Tt}^{(i)}$ of the i-th system) are introduced. Then, equation (24) can be re-written in a scalar form:

$$\begin{aligned} \dot{g}_N^{(i)} &= \tilde{n}_i^T J_{gC_i} \underline{\dot{s}}_{C_i} + \tilde{n}_i^T J_{g\pi_i} \underline{\dot{s}}_{\pi_i}, \\ \dot{g}_{Tl}^{(i)} &= \tilde{t}_{l_i}^T J_{gC_i} \underline{\dot{s}}_{C_i} + \tilde{t}_{l_i}^T J_{g\pi_i} \underline{\dot{s}}_{\pi_i}, \quad i \in \Omega_S^* \\ \dot{g}_{Tt}^{(i)} &= \tilde{t}_{t_i}^T J_{gC_i} \underline{\dot{s}}_{C_i} + \tilde{t}_{t_i}^T J_{g\pi_i} \underline{\dot{s}}_{\pi_i} \end{aligned} \qquad (25)$$

where $J_{gC_i}, J_{g\pi_i}$ are the 3×3 Jacobian matrices defined in (24). The motion of the constraint surface $\underline{\dot{s}}_{\pi_i}$ (in the case when it is mobile) is either prescribed or calculated from a separate mathematical model of the object (constraint). If the following kinematic relations are introduced:

$$\underline{s}_{C_i} = \underline{s}_{C_i}(Q,t), \quad i \in \Omega_S^* \qquad (26)$$

$$\underline{\dot{s}}_{C_i} = J_{C_i}(Q)\dot{Q}, \quad i \in \Omega_S^* \qquad (27)$$

then equations (25) can be expanded to acquire the form:

$$\begin{aligned} \dot{g}_N^{(i)} &= \tilde{n}_i^T J_{gC_i} J_{C_i}(Q) \cdot \dot{Q} + \tilde{n}_i^T J_{g\pi_i} \underline{\dot{s}}_{\pi_i} = \\ &= J_{gC_i,TOT}^N \dot{Q} + A_{g\pi_i}^N, \end{aligned}$$

$$\begin{aligned} \dot{g}_{Tl}^{(i)} &= \tilde{t}_{l_i}^T J_{gC_i} J_{C_i}(Q) \cdot \dot{Q} + \tilde{t}_{l_i}^T J_{g\pi_i} \underline{\dot{s}}_{\pi_i} = \\ &= J_{gC_i,TOT}^{Tl} \dot{Q} + A_{g\pi_i}^{Tl}, \end{aligned} \qquad i \in \Omega_S^* \quad (28)$$

$$\begin{aligned} \dot{g}_{Tt}^{(i)} &= \tilde{t}_{t_i}^T J_{gC_i} J_{C_i}(Q) \cdot \dot{Q} + \tilde{t}_{t_i}^T J_{g\pi_i} \underline{\dot{s}}_{\pi_i} = \\ &= J_{gC_i,TOT}^{Tt} \dot{Q} + A_{g\pi_i}^{Tt} \end{aligned}$$

where $J_{C_i} = \dfrac{\partial \underline{s}_{C_i}(Q)}{\partial Q}$ is a $(3 \times N)$ Jacobian matrix defining the dependence of the linear velocity $\underline{\dot{s}}_{C_i}$ of the i-th point C_i as a function of the generalized coordinates $\dot{Q}$; $J_{gC_i,TOT}^N = \tilde{n}_i^T J_{gC_i} J_{C_i}(Q)$, $J_{gC_i,TOT}^{Tl} = \tilde{t}_{l_i}^T J_{gC_i} J_{C_i}(Q)$ and $J_{gC_i,TOT}^{Tt} = \tilde{t}_{t_i}^T J_{gC_i} J_{C_i}(Q)$ are the $(1 \times N)$ total Jacobian matrices; $A_{g\pi_i}^N = \tilde{n}_i^T J_{g\pi_i} \underline{\dot{s}}_{\pi_i}$, $A_{g\pi_i}^{Tl} = \tilde{t}_{l_i}^T J_{g\pi_i} \underline{\dot{s}}_{\pi_i}$ and

$A_{g\pi_i}^{Tt} = \tilde{t}_{t_i}^T J_{g\pi_i} \underline{\dot{s}}_{\pi_i}$ are the corresponding adjoint scalars from (28).

Taking into account the previous consideration, as well as the contact force vector (22), the contact-dynamics model (13) can be rewritten in the form that includes multi-point contact effects:

$$H\ddot{Q} + \tilde{h} - \sum_{i\in\Omega_S^*} J_{gC_i,TOT}^{N}{}^T \cdot F_{N_i} - \sum_{i\in\Omega_S^*} J_{gC_i,TOT}^{Tl}{}^T \cdot F_{Tl_i} - $$
$$- \sum_{i\in\Omega_S^*} J_{gC_i,TOT}^{Tt}{}^T \cdot F_{Tt_i} = \underline{0} \qquad (29)$$

where $\tilde{h} = h - \tau$ is an $(N\times1)$ vector taking into account the gravity and centrifugal effects, as well as the driving torques at the biped joints. Kinematic and dynamic relations (28) and (29) represent the basis for the development of the impact model of the biped gait. Let us write them in a matrix notation:

$$\begin{bmatrix} \underline{\dot{g}}_N \\ \underline{\dot{g}}_{Tl} \\ \underline{\dot{g}}_{Tt} \end{bmatrix} = \begin{bmatrix} W_N \\ W_{Tl} \\ W_{Tt} \end{bmatrix} \dot{Q} + \begin{bmatrix} \tilde{\omega}_N \\ \tilde{\omega}_{Tl} \\ \tilde{\omega}_{Tt} \end{bmatrix} \qquad (30)$$

$$H\ddot{Q} + \tilde{h} - \begin{bmatrix} W_N^T & W_{Tl}^T & W_{Tt}^T \end{bmatrix} \cdot \begin{bmatrix} F_N \\ F_{Tl} \\ F_{Tt} \end{bmatrix} = \underline{0} \qquad (31)$$

where: $\underline{\dot{g}}_N = \begin{bmatrix} \dot{g}_N^{(1)} & \cdots & \dot{g}_N^{(n_S^*)} \end{bmatrix}^T$, $\underline{\dot{g}}_{Tl} = \begin{bmatrix} \dot{g}_{Tl}^{(1)} & \cdots & \dot{g}_{Tl}^{(n_S^*)} \end{bmatrix}^T$,

$\underline{\dot{g}}_{Tt} = \begin{bmatrix} \dot{g}_{Tt}^{(1)} & \cdots & \dot{g}_{Tt}^{(n_S^*)} \end{bmatrix}^T$ are $\left(n_S^*\times1\right)$ integrated vectors of the relative body (foot) velocities in the normal and tangential coordinate directions of motion; $W_N = \begin{bmatrix} J_{gC_1,TOT}^N \cdots J_{gC_{n_S^*},TOT}^N \end{bmatrix}^T$, $W_{Tl} = \begin{bmatrix} J_{gC_1,TOT}^{Tl} \cdots J_{gC_{n_S^*},TOT}^{Tl} \end{bmatrix}^T$

and $W_{Tt} = \begin{bmatrix} J_{gC_1,TOT}^{Tt} \cdots J_{gC_{n_S^*},TOT}^{Tt} \end{bmatrix}^T$ are the Jacobian matrices determined for the motions in the normal and tangential directions; $\tilde{\omega}_N = \begin{bmatrix} A_{g\pi_1}^N \cdots A_{g\pi_{n_S^*}}^N \end{bmatrix}^T$, $\tilde{\omega}_{Tl} = \begin{bmatrix} A_{g\pi_1}^{Tl} \cdots A_{g\pi_{n_S^*}}^{Tl} \end{bmatrix}^T$,

$\tilde{\omega}_{Tt} = \begin{bmatrix} A_{g\pi_1}^{Tt} \cdots A_{g\pi_{n_S^*}}^{Tt} \end{bmatrix}^T$ are $\left(n_S^*\times1\right)$ vectors of the adjoint scalars defined in the kinematic relations (30); $F_N = \begin{bmatrix} F_{N_1} \cdots F_{N_{n_S^*}} \end{bmatrix}^T$, $F_{Tl} = \begin{bmatrix} F_{Tl_1} \cdots F_{Tl_{n_S^*}} \end{bmatrix}^T$, $F_{Tt} = \begin{bmatrix} F_{Tt_1} \cdots F_{Tt_{n_S^*}} \end{bmatrix}^T$ are $\left(n_S^*\times1\right)$ vectors of normal and tangential impact forces.

After integrating equation (31) over the impact period $\Delta t_{c_i} = t_{c_i}'' - t_{c_i}', i\in\Omega_S^*$, the following expression is derived:

$$H(\dot{Q}'' - \dot{Q}') - \begin{bmatrix} W_N^T & W_{Tl}^T & W_{Tt}^T \end{bmatrix} \cdot \begin{bmatrix} \Lambda_N(t_c') \\ \Lambda_{Tl}(t_c') \\ \Lambda_{Tt}(t_c') \end{bmatrix} = \underline{0} \quad (32)$$

Here $\Lambda_N(t_c'), \Lambda_{Tl}(t_c'), \Lambda_{Tt}(t_c')$ are the impulse momentums in the normal and tangential directions which are transferred during the impact. They can be defined in the following way:

$$\Lambda_N = \begin{bmatrix} F_{N_1}\Delta t_{c_1}, \dots F_{N_{n_S^*}}\Delta t_{c_{n_S^*}} \end{bmatrix}^T,$$
$$\Lambda_{Tl} = \begin{bmatrix} F_{Tl_1}\Delta t_{c_1}, \dots F_{Tl_{n_S^*}}\Delta t_{c_{n_S^*}} \end{bmatrix}^T,$$
$$\Lambda_{Tt} = \begin{bmatrix} F_{Tt_1}\Delta t_{c_1}, \dots F_{Tt_{n_S^*}}\Delta t_{c_{n_S^*}} \end{bmatrix}^T$$

Knowing that $\dot{Q}' = \dot{Q}(t_c')$ and $\dot{Q}'' = \dot{Q}(t_c'')$ are the instances of start and termination of the impact, the relative velocities at these instants can be defined:

$$\begin{bmatrix} \underline{\dot{g}}_N(t_c') \\ \underline{\dot{g}}_{Tl}(t_c') \\ \underline{\dot{g}}_{Tt}(t_c') \end{bmatrix} = \begin{bmatrix} W_N \\ W_{Tl} \\ W_{Tt} \end{bmatrix} \dot{Q}' + \begin{bmatrix} \tilde{\omega}_N \\ \tilde{\omega}_{Tl} \\ \tilde{\omega}_{Tt} \end{bmatrix};$$
$$\begin{bmatrix} \underline{\dot{g}}_N(t_c'') \\ \underline{\dot{g}}_{Tl}(t_c'') \\ \underline{\dot{g}}_{Tt}(t_c'') \end{bmatrix} = \begin{bmatrix} W_N \\ W_{Tl} \\ W_{Tt} \end{bmatrix} \dot{Q}'' + \begin{bmatrix} \tilde{\omega}_N \\ \tilde{\omega}_{Tl} \\ \tilde{\omega}_{Tt} \end{bmatrix} \qquad (33)$$

From the relations defined in (33), it is possible to derive the following functional dependence between the relative velocities in two characteristic instances t_c' and t_c'' of the impact. Then:

$$\begin{bmatrix} \underline{\dot{g}}_N(t_c'') \\ \underline{\dot{g}}_{Tl}(t_c'') \\ \underline{\dot{g}}_{Tt}(t_c'') \end{bmatrix} = \begin{bmatrix} W_N \\ W_{Tl} \\ W_{Tt} \end{bmatrix}(\dot{Q}'' - \dot{Q}') + \begin{bmatrix} \underline{\dot{g}}_N(t_c') \\ \underline{\dot{g}}_{Tl}(t_c') \\ \underline{\dot{g}}_{Tt}(t_c') \end{bmatrix} \qquad (34)$$

Expressing the $\dot{Q}' - \dot{Q}''$ from (32) and including it in (34), the model of the unilateral multi-point impact of the biped locomotion system is derived:

$$\begin{bmatrix} \underline{\dot{g}}_N(t_c'') \\ \underline{\dot{g}}_{Tl}(t_c'') \\ \underline{\dot{g}}_{Tt}(t_c'') \end{bmatrix} = \begin{bmatrix} W_N \\ W_{Tl} \\ W_{Tt} \end{bmatrix} H^{-1} \begin{bmatrix} W_N^T & W_{Tl}^T & W_{Tt}^T \end{bmatrix} \cdot \begin{bmatrix} \Lambda_N(t_c') \\ \Lambda_{Tl}(t_c') \\ \Lambda_{Tt}(t_c') \end{bmatrix} +$$
$$+ \begin{bmatrix} \underline{\dot{g}}_N(t_c') \\ \underline{\dot{g}}_{Tl}(t_c') \\ \underline{\dot{g}}_{Tt}(t_c') \end{bmatrix} \qquad (35)$$

The model (35) consists of $3n_S^*$ scalar equations for $6n_S^*$ unknowns. Thus, $3n_s$ conditions must yet be formulated in order to determine the transferred impulses $\Lambda_N(t_c'), \Lambda_{Tl}(t_c'), \Lambda_{Tt}(t_c')$ and the relative velocities $\underline{\dot{g}}_N(t_c''), \underline{\dot{g}}_{Tl}(t_c''), \underline{\dot{g}}_{Tt}(t_c'')$ at the end of the impact.

The normal impulse of compression results from integration of the normal force over the phase of compression:

$$\Lambda_{N_i} = \lim_{t_{c_i}'' \to t_{c_i}^*} \int_{t_{C_i}'}^{t_{C_i}''} F_{N_i} \, dt, \quad i\in\Omega_S^* \qquad (36)$$

where, due to the unilateral character of contact constraint, only compressive forces are possible:

$$F_{N_i}(t) \geq 0 \quad \forall \quad t\in[t_{c_i}', t_{c_i}''] \qquad (37)$$

Thus, integrating (36) the normal forces with the property (37) results in non-negative values of the normal impulses:

$$\Lambda_{N_i} \geq 0, \quad i \in \Omega_S^* \tag{38}$$

If the impulse (38) is transferred, then the corresponding contact participates in the impact and the end of compression is given by $\dot{g}_N^{(i)} = 0$. Thus, the allowed velicities correspond to $\dot{g}_N^{(i)} \geq 0$. The overall behavior can be expressed by the single complementarity condition [12, 13]:

$$\begin{aligned} \Lambda_{N_i} \geq 0; \quad \dot{g}_N^{(i)} \geq 0; \\ \Lambda_{N_i} \dot{g}_N^{(i)} = 0; \quad i \in \Omega_S^* \end{aligned} \tag{39}$$

The model (35) should be supplemented by Coulomb's friction law. The tangential impulse can be derived in a similar way as equation (36), by integration:

$$\Lambda_{Tl_i} = \lim_{t'_{c_i} \to t''_{c_i}} \int_{t'_{C_i}}^{t''_{c_i}} F_{Tl_i}\, dt; \quad \Lambda_{Tt_i} = \lim_{t'_{c_i} \to t''_{c_i}} \int_{t'_{c_i}}^{t''_{c_i}} F_{Tt_i}\, dt; \quad i \in \Omega_S^* \tag{40}$$

Now, we state a tangential impact law in the longitudinal direction $g_{Tl}^{(i)}$ as [12]:

$$\begin{aligned} &\left| \Lambda_{Tl_i} \right| \leq \mu_i \Lambda_{N_i}; \quad i \in \Omega_S^* \\ &\begin{cases} \left| \Lambda_{Tl_i} \right| < \mu_i \Lambda_{N_i} &\Rightarrow \dot{g}_{Tl}^{(i)} = 0 \quad \text{case of stiction} \\ \Lambda_{Tl_i} = +\mu_i \Lambda_{N_i} &\Rightarrow \dot{g}_{Tl}^{(i)} \leq 0 \quad \text{case of friction} \\ \Lambda_{Tl_i} = -\mu_i \Lambda_{N_i} &\Rightarrow \dot{g}_{Tl}^{(i)} \geq 0 \quad \text{case of friction} \end{cases} \end{aligned} \tag{41}$$

as well as in the transversal direction $g_{Tt}^{(i)}$:

$$\begin{aligned} &\left| \Lambda_{Tt_i} \right| \leq \mu_i \Lambda_{N_i}; \quad i \in \Omega_S^* \\ &\begin{cases} \left| \Lambda_{Tt_i} \right| < \mu_i \Lambda_{N_i} &\Rightarrow \dot{g}_{Tt}^{(i)} = 0 \quad \text{case of stiction} \\ \Lambda_{Tt_i} = +\mu_i \Lambda_{N_i} &\Rightarrow \dot{g}_{Tt}^{(i)} \leq 0 \quad \text{case of friction} \\ \Lambda_{Tt_i} = -\mu_i \Lambda_{N_i} &\Rightarrow \dot{g}_{Tt}^{(i)} \geq 0 \quad \text{case of friction} \end{cases} \end{aligned} \tag{42}$$

Also, the dissipative character of eqs. (41) and (42) should be stressed out:

$$\Lambda_{Tl_i} \dot{g}_{Tl}^{(i)} \leq 0; \quad \Lambda_{Tt_i} \dot{g}_{Tt}^{(i)} \leq 0; \quad i \in \Omega_S^* \tag{43}$$

Thus (41) and (42) should be regarded as independent tangential impact laws in two orthogonal tangential directions (longitudinal and transversal) which coincide with Coulomb's friction law [12] and contain all the main physical effects of dry friction. With (39), (41) and (42) the missing $3n_S^*$ impact conditions are found and the problem is closed in a mathematical sense, i.e. the number of unknows in the model (36) is equal to its order.

The dynamic equations (32), (41), (42), together with the corresponding kinematic relations (34) of the system, can be stated as an LCP formulation. Because of the system discontinuity (expressed by eqs. (41) and (42)), due to the non-smooth stiction/friction characteristics, the LCP approach should be applied to both directions - the normal and the tangential. Initially, this demands decomposition of the friction characteristics (41) and (42), i.e. the decomposition of tangential characteristics according to [12, 13]. The basic idea for decomposing friction characteristic is to formulate each of the tangential constraints by two simultaneously appearing constraints. Each of them transfers only one part of it. Both constraints transmit the tangential force F_{Tli} (F_{Tti}) by splitting it into

the portions $F_{Tl}^{(+)}$ and $F_{Tl}^{(-)}$ ($F_{Tt}^{(+)}$ and $F_{Tt}^{(-)}$) in the positive and negative tangential directions [12], respectively. Then, the state F_{Tli} (F_{Tti}) can be written in the folowing way:

$$\begin{aligned} F_{Tl_i} = F_{Tl_i}^{(+)} - F_{Tl_i}^{(-)}, \quad i \in \Omega_{H_1} \\ F_{Tt_i} = F_{Tt_i}^{(+)} - F_{Tt_i}^{(-)}, \quad i \in \Omega_{H_2} \end{aligned} \tag{44}$$

The values $F_{Tl}^{(+)}$ and $F_{Tl}^{(-)}$ ($F_{Tt}^{(+)}$ and $F_{Tt}^{(-)}$) are not arbitrary but must be chosen in such a manner that the tangential force F_{Tli} (F_{Tti}) always lies in the convex set C_{Tl_i} (C_{Tt_i}) defined in the following way. The admissible values of the tangential forces F_{Tli} and F_{Tti} form the convex sets C_{Tl_i} and C_{Tt_i} which are bounded by the values of the normal force [12]:

$$\begin{aligned} C_{Tl_i} &= \left\{ F_{Tl_i} \mid -\mu_i F_{N_i} \leq F_{Tl_i} \leq +\mu F_{N_i} \right\}, \\ C_{Tt_i} &= \left\{ F_{Tt_i} \mid -\mu_i F_{N_i} \leq F_{Tt_i} \leq +\mu F_{N_i} \right\}, \\ i &\in \Omega_S \end{aligned} \tag{45}$$

If the tangential forces F_{Tli} and F_{Tti} are in the interior of the sets C_{Tl_i} and C_{Tt_i}, then the continual sticking appears in both directions (the longitudinal $\dot{g}_{Tl}^{(i)} = 0$, $\ddot{g}_{Tl}^{(i)} = 0$ and the transversal $\dot{g}_{Tt}^{(i)} = 0$, $\ddot{g}_{Tt}^{(i)} = 0$). Otherwise, the tangential forces F_{Tli} and F_{Tti} lie at the boundaries of C_{Tl_i} and C_{Tt_i} and allow transition to sliding by arbitrary values of $\ddot{g}_{Tl}^{(i)}$ and $\ddot{g}_{Tt}^{(i)}$ in the oposing directions. This can be ensured by restricting the values of $F_{Tl}^{(+)}$ and $F_{Tl}^{(-)}$ ($F_{Tt}^{(+)}$ and $F_{Tt}^{(-)}$) to

$$\begin{aligned} F_{Tl_i}^{(+)} &\in C_{Tl_i}^{(+)} = \left\{ F_{Tl_i}^{(+)} \mid 0 \leq F_{Tl_i}^{(+)} \leq \mu_i F_{N_i} \right\}, \\ F_{Tl_i}^{(-)} &\in C_{Tl_i}^{(-)} = \left\{ F_{Tl_i}^{(-)} \mid -\mu_i F_{N_i} \leq F_{Tl_i}^{(-)} \leq 0 \right\}, \quad i \in \Omega_{H_1} \\ F_{Tt_i}^{(+)} &\in C_{Tt_i}^{(+)} = \left\{ F_{Tt_i}^{(+)} \mid 0 \leq F_{Tt_i}^{(+)} \leq \mu_i F_{N_i} \right\}, \\ F_{Tt_i}^{(-)} &\in C_{Tt_i}^{(-)} = \left\{ F_{Tt_i}^{(-)} \mid -\mu_i F_{N_i} \leq F_{Tt_i}^{(-)} \leq 0 \right\}, \quad i \in \Omega_{H_2} \end{aligned} \tag{46}$$

For each of the new variables $F_{Tl}^{(+)}$ and $F_{Tl}^{(-)}$ ($F_{Tt}^{(+)}$ and $F_{Tt}^{(-)}$) the connections to the tangential relative acceleration $\ddot{g}_{Tl}^{(i)}$ ($\ddot{g}_{Tt}^{(i)}$) should be defined in order to bring the system to the LCP formulation. Fig.4 presents the decomposition of the friction characteristic (the longitudinal commponent) according to [12]. Similar graphs are obtained for the characteristic in the transversal direction but they are not depicted separately.

The decomposition shown in Fig.4 enables the LCP formulation by using the resulting inequlities and complementarity conditions, together with the dynamic equations derived previously. Following the decomposition procedure shown in Figures 4c and 4d one obtains [12]:

$$\begin{aligned} \ddot{g}_{Tl_i} &= z_i^+ - \ddot{g}_{Tl_i}^- \\ \ddot{g}_{Tl_i} &= \ddot{g}_{Tl_i}^+ - z_i^- \\ F_{Tl0_i}^{(+)} &= \mu_i F_{N_i} - F_{Tl_i}^{(-)} \\ F_{Tl0_i}^{(-)} &= \mu_i F_{N_i} - F_{Tl_i}^{(+)} \end{aligned} \quad i \in \Omega_{H_1} \tag{47}$$

Similar relations can also be written for the accelerations and tangential forces in the transversal direction. The physical meaning of the auxilary variables z_i^+ and z_i^- is

obvious by this set of equations. They denote just the positive as well as the negative parts of accelerations, and they have been introduced merely for the reason of distinction. From (47), the following equivalencies hold: $z_i^+ = \ddot{g}_{Tl_i}^+$, $z_i^- = \ddot{g}_{Tl_i}^-$. The terms $F_{Tl0_i}^{(+)}$ and $F_{Tl0_i}^{(-)}$ are called friction saturations (in the longitudinal direction) and stand for the differences of the maximal transferable and actual tangential forces. When they vanish, a transition to sliding is possible. Finally, the complementarity conditions, that are presented in Fig.4d, can be defined in the following way:

a)

b)

c)

d)
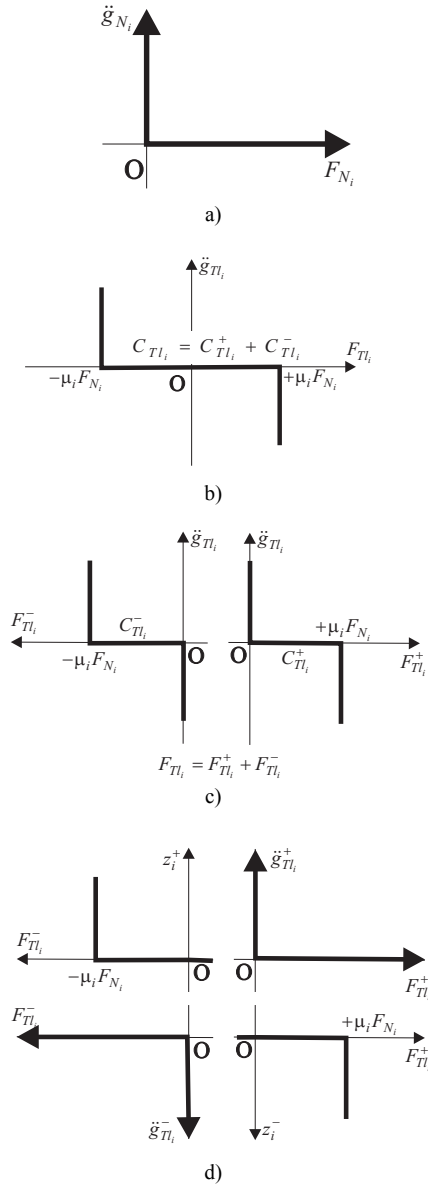
Figure 4. a) Complementarity of normal contacts; b) Friction characteristics during contact; c), d) Decomposition of the friction characteristic in two steps [12]

$$
\begin{aligned}
\ddot{g}_{Tl_i}^- \geq 0; \quad F_{Tl_i}^- \geq 0; \quad \ddot{g}_{Tl_i}^- F_{Tl_i}^- = 0 \\
\ddot{g}_{Tl_i}^+ \geq 0; \quad F_{Tl_i}^+ \geq 0; \quad \ddot{g}_{Tl_i}^+ F_{Tl_i}^+ = 0 \\
F_{Tl0_i}^+ \geq 0; \quad z_i^+ \geq 0; \quad F_{Tl0_i}^+ z_i^+ = 0 \\
F_{Tl0_i}^- \geq 0; \quad z_i^- \geq 0; \quad F_{Tl0_i}^- z_i^- = 0
\end{aligned} \quad i \in \Omega_{H1} \quad (48)
$$

The set of relations (48) describes in full the decomposed friction characteristics which correspond to four unilateral constraints. Equations (44) - (48) have to be used for each of the potentially sticking contacts $i \in \Omega_{H1}$.

Now, the impact model is fully determined by the corresponding kinetics (32) and kinematics equation (34) of the biped locomotion system, the impact law in the normal direction (39), and the tangential impact characteristics (41) and (42). In order to determine the model unknowns (the transferred impact impulses $\Lambda_N(t_c'), \Lambda_{Tl}(t_c'), \Lambda_{Tt}(t_c')$, as well as the impact velocities $\dot{\underline{g}}_N(t_c''), \dot{\underline{g}}_{Tl}(t_c''), \dot{\underline{g}}_{Tt}(t_c'')$) the LCP formulation will be applied [12,13]. For that purpose, because of the non-smoothness and discontinuity of the friction dynamics, the decomposition of the tangential relative velocities $\dot{\underline{g}}_{Tl}(t_c''), \dot{\underline{g}}_{Tt}(t_c'')$ and tangential impact impulses $\Lambda_{Tl}(t_c'), \Lambda_{Tt}(t_c')$ is performed in a way described by (44)-(48) [12]. Finally, the impact model of the biped gait is defined in an LCP form. For establishing equations for the LCP, (44), (47) and (48) should be integrated over the impact interval Δt. Then the following relations are obtained:

$$
\begin{aligned}
\Lambda_{Tl_i} = \Lambda_{Tl_i}^{(+)} - \Lambda_{Tl_i}^{(-)}, \quad i \in I_{H1} \\
\dot{g}_{Tl_i} = z_i^+ - \dot{g}_{Tl_i}^-; \quad \Lambda_{Tl0_i}^{(+)} = \Lambda_{G_i}^{(-)} - \Lambda_{Tl_i}^{(-)}; \quad i \in \Omega_{H1} \\
\dot{g}_{Tl_i} = \dot{g}_{Tl_i}^+ - z_i^-; \quad \Lambda_{Tl0_i}^{(-)} = \Lambda_{G_i}^{(+)} - \Lambda_{Tl_i}^{(+)};
\end{aligned} \quad (49)
$$

and

$$
\begin{aligned}
\dot{g}_{Tl_i}^- \geq 0; \quad \Lambda_{Tl_i}^{(-)} \geq 0; \quad \dot{g}_{Tl_i}^- \Lambda_{Tl_i}^{(-)} = 0 \\
\dot{g}_{Tl_i}^+ \geq 0; \quad \Lambda_{Tl_i}^{(+)} \geq 0; \quad \dot{g}_{Tl_i}^+ \Lambda_{Tl_i}^{(+)} = 0 \\
\Lambda_{Tl0_i}^{(+)} \geq 0; \quad z_i^+ \geq 0; \quad \Lambda_{Tl0_i}^{(+)} z_i^+ = 0 \\
\Lambda_{Tl0_i}^{(-)} \geq 0; \quad z_i^- \geq 0; \quad \Lambda_{Tl0_i}^{(-)} z_i^- = 0
\end{aligned} \quad i \in \Omega_{H1} \quad (50)
$$

All tangential impulses Λ_{Tl} of the impact contacts $i \in \Omega_S^*$ can be defined as a vector difference:

$$
\begin{aligned}
\Lambda_{Tl} = \Lambda_{Tl}^{(+)} - \Lambda_{Tl}^{(-)}; \\
\Lambda_{Tl}^{(+)} = \left[\Lambda_{Tl_1}^{(+)} \dots \Lambda_{Tl_{n_S^*}}^{(+)} \right]^T; \\
\Lambda_{Tl}^{(-)} = \left[\Lambda_{Tl_1}^{(-)} \dots \Lambda_{Tl_{n_S^*}}^{(-)} \right]^T
\end{aligned} \quad (51)
$$

Then, taking into account eqs. (32) and (34), the following LCP relation can be derived:

$$
\begin{bmatrix} \dot{g}_C \\ \Lambda_{T0_C} \end{bmatrix} = \begin{bmatrix} W_S^T H^{-1} W_S & I_S^T \\ N_S - I_S & \underline{0} \end{bmatrix} \cdot \begin{bmatrix} \Lambda_C \\ z_C \end{bmatrix} + \begin{bmatrix} \dot{g}_A \\ \underline{0} \end{bmatrix}
$$

$$
\begin{bmatrix} \dot{g}_C \\ \Lambda_{T0_C} \end{bmatrix} \geq \underline{0}; \quad \begin{bmatrix} \Lambda_C \\ z_C \end{bmatrix} \geq \underline{0}; \quad \begin{bmatrix} \dot{g}_C \\ \Lambda_{T0_C} \end{bmatrix}^T \cdot \begin{bmatrix} \Lambda_C \\ z_C \end{bmatrix} = \underline{0};
$$

(52)

where the matrices and vectors used have the forms:

$$
\dot{\underline{g}}_C = \begin{bmatrix} \dot{\underline{g}}_N \\ +\dot{\underline{g}}_{Tl} \\ +\dot{\underline{g}}_{Tt} \\ -\dot{\underline{g}}_{Tl} \\ -\dot{\underline{g}}_{Tt} \end{bmatrix}; \quad \dot{\underline{g}}_A = \begin{bmatrix} \dot{\underline{g}}_N \\ \dot{\underline{g}}_{Tl}^+ \\ \dot{\underline{g}}_{Tt}^+ \\ \dot{\underline{g}}_{Tl}^- \\ \dot{\underline{g}}_{Tt}^- \end{bmatrix};
$$

$$z_C = \begin{bmatrix} z_C^- \\ z_C^+ \end{bmatrix} = \begin{bmatrix} \dot{g}_{Tl}^- \\ \dot{g}_{Tt}^- \\ \dot{g}_{Tl}^+ \\ \dot{g}_{Tt}^+ \end{bmatrix}; \quad \Lambda_C = \begin{bmatrix} \Lambda_N \\ \Lambda_{Tl}^{(+)} \\ \Lambda_{Tt}^{(+)} \\ \Lambda_{Tl}^{(-)} \\ \Lambda_{Tt}^{(-)} \end{bmatrix};$$

$$W_S = \begin{bmatrix} W_N^T \\ +W_{Tl}^T \\ +W_{Tt}^T \\ -W_{Tl}^T \\ -W_{Tt}^T \end{bmatrix}; \quad I_S^T = \begin{bmatrix} \underline{0} & \underline{0} & \underline{0} & \underline{0} \\ \underline{E} & \underline{0} & \underline{0} & \underline{0} \\ \underline{0} & \underline{E} & \underline{0} & \underline{0} \\ \underline{0} & \underline{0} & \underline{E} & \underline{0} \\ \underline{0} & \underline{0} & \underline{0} & \underline{E} \end{bmatrix};$$

$$N_S - I_S = \begin{bmatrix} \overline{\mu}_S & -E & \underline{0} & \underline{0} & \underline{0} \\ \underline{\mu}_S & \underline{0} & -E & \underline{0} & \underline{0} \\ \underline{\mu}_S & \underline{0} & \underline{0} & -E & \underline{0} \\ \underline{\mu}_S & \underline{0} & \underline{0} & \underline{0} & -E \end{bmatrix}$$

$$\Lambda_{T0C} = \begin{bmatrix} \Lambda_{Tl0}^{(-)} \\ \Lambda_{Tt0}^{(-)} \\ \Lambda_{Tl0}^{(+)} \\ \Lambda_{Tt0}^{(+)} \end{bmatrix} = \begin{bmatrix} \Lambda_{T0C}^{(-)} \\ \Lambda_{T0C}^{(+)} \end{bmatrix} = (N_S - I_S) \cdot \Lambda_C$$

$E \in \Re^{n_S^* \times n_S^*}$ is a unit matix and $\overline{\mu}_S \in \Re^{n_S^* \times n_S^*}$ is a diagonal matrix consisting of the coefficients of friction μ_i. The dimensions of the vectors and matrices used in (52) are: $\dot{g}_N$, $\dot{g}_A$, $\Lambda_C \in \Re^{5n_S^* \times 1}$, $W_S \in \Re^{N \times 5n_S^*}$, Λ_{T0C}, $z_C \in \Re^{4n_S^* \times 1}$.

Relation (52) represents the standard LCP formulation of the impact law that can be written in a general form:

$$y = Ax + b; \quad y \geq \underline{0}; \quad x \geq \underline{0}; \quad y^T x = \underline{0}$$
$$y, x \in R^{5n_S} \tag{53}$$

Its solution $y \in \Re^{5n_S}$, $x \in \Re^{5n_S}$ contains all unkonown contact impulses and velocities during the impact. Lemke's algorithm [19] can be used as an efficient numerical solver of (53).

Experimental Background and Simulation

With the aim of identifying a valid model of the biped locomotion system of the anthropomorphic structure, experiments were carried out in a caption motion studio. For this purpose, a middle-aged (36) male subject, 190 cm tall, weighing 84.0728 kg, of normal physical constitution and functionality, played the role of an experimental antropomorphic system whose model was to be identified. The subject's geometrical parameters (the lengths of the links, the distances between the neighboring joints and the particular significant points on the body) were determined by direct measurements or photometrically. The other kinematic parameters, as well as dynamic ones, were determined on the basis of the tables, recommendations and empirical relations given in [20, 21], which resulted from the biometric measurements on a broad human population. The selected subject, whose parameters were identified, performed a number of motion tests (walking, staircase climbing, jumping), whereby the measurements were made

under the appropriate laboratory conditions. The characteristic laboratory details are shown in Fig.5. The VICON-460 caption motion studio equipment was used with the corresponding software package for processing measurement data. To detect positions of the body links fluorescent markers where placed at the characteristic points of the body (Figures 5a and 5b). Continual monitoring of the position markers during the motion was performed using six Vicon high-accuracy infra-red cameras with the recording frequency of 200 Hz (Fig.5c). Reactive forces of the foot impact/contact with the ground were measured on the force platform (Fig.5d) with a recording frequency of 1.0 Khz. To mimic a rigid foot-ground contact a 5-mm thick wooden plate was fixed to each foot (Fig.5b). This yielded significant neutralization of the elastic effects due to the rubber footsole and realization of a quasi-rigid contact of the foot and the ground.

A moderately fast walk ($v = 1.25$ [m/s]) was considered as a typical example of a contact task which encompasses all the elements of the phenomenon of mechanical impact and regular foot-ground contact. Reactive forces and moments measured on the right foot in its stepping on the measurement platform in the experimental walk are shown in Fig.6. Having in mind the experimental measurements on the biological system and, based on them further theoretical considerations, we assumed that it is possible to design a bipedal locomotion mechanism of a similar anthropomorphic structure and with defined (geometric and dynamic) parameters. However, at the present level of technological development this is not possible, first of all because of the lack of adequate actuators. Still, in theoretical considerations, this assumption is taken as conditionally true, presuming that the technological advancement will soon enable the synthesis of artificial muscles that look like the human ones. In this way, the research problem is placed in the frame of mechanics of rigid bodies, using the available mathematical apparatus appropriate for this scientific discipline.

a)

b)

c)

d)

Figure 5: Experimental capture motion studio in the Laboratory of Biomechanics (University of La Reunion, CURAPS, Le Tampon, France): a) Measurements of human motion using fluorescent markers attached to a human body; b) Wooden plates as the feet soles used in locomotion experiments; c) Vicon infra-red camera used to capture the human motion; d) 6-DOFs force sensing platform – sensor distribution at the back side of the plate

The objective of this section is to demonstrate how the application of theoretical results (mathematic model) presented in Section 2.1 gives the possibility to reproduce the physical behavior of a biological system (human) with a relatively high accuracy. In this sense, we started from the assumption that the system parameters were determined with a satisfactory accuracy and that they reflect faithfully characteristics of the biological system.
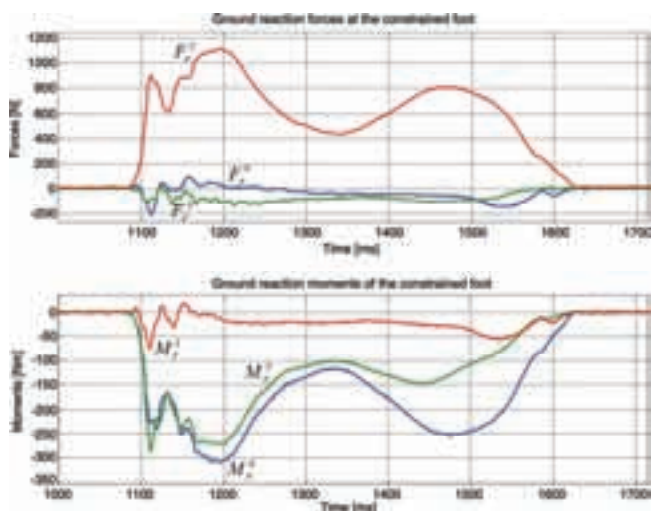
Figure 6: Experimentally measured ground reaction forces and moments on the right foot of the subject under laboratory conditions (Fig.5)

Bearing in mind mechanical complexity of the structure of the human body, with its numerous DOFs, we adopted the corresponding kinematic structure (scheme) of the biped locomotion mechanism (Fig.7) to be used in the sequel. We have proved through the simulation results that the complexity of the model shown in Fig.7 is capable to reproduce with a relatively high accuracy any anthropomorphic motion – dynamic gait, climbing and descending the staircase, jumping, etc. The adopted structure has three active mechanical DOFs at each of the joints - the hip, waist, shoulders and neck; two at the ankle and wrist, and one at the knee, elbow and toe. The fact is that not all available mechanical DOFs are needed in different anthropomorphic movements. In the example considered in this work we defined the nominal motion of the joints of the legs and of the trunk. At the same time, the joints of the arms, neck and toes remained immobilized. On the basis of the measured values of positions (coordinates) of fluorescent markers in the course of motion (Figures 5a, 5b) it was possible to identify angular trajectories of the particular joints of the bipedal locomotion system. The identified trajectories of the system's joints were differentiated with respect to time, with a sampling period of $\Delta t = 0.001\,[\text{ms}]$. In this way, the corresponding vectors of angular velocities and angular accelerations at the joints of the system were determined.
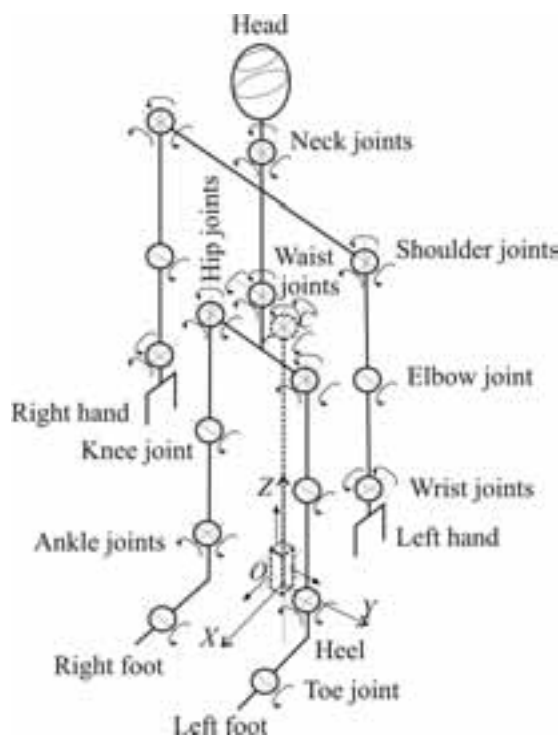
Figure 7. Kinematic scheme of a 38-DOF biped locomotion system used in simulation as the kinematic model of the human body referred to in the experiments

Animation of the gait of the biped locomotion system shown in Fig.7, for the identified joint trajectories, is presented in Fig.8 through the several characteristic positions. The motion simulation shown in Fig.8 was determined using a kinematic model of the system [6].

The biped starts from the state of rest and then makes four half-steps stepping with the right foot on the platform for force measurement. Feet of the biped mechanism in particular moments strike the support. Simulation of the kinematic and dynamic models was performed using Matlab and [23, 24].

The mechanism feet describe their own trajectories (cycloids) in the Cartesian coordinate system by passing from the state of contact with the ground (zero position) to free motion state (position above zero, Fig.9). The functional coordinates (Fig.3), defining the relative position of the foot contour points with respect to the constraint surface π, change their values alternately in accordance with the motion of the right and the left leg (Fig.9). The hodographs of the functional movements of the coordinates of contour points on the left and right feet (calculated on the basis of the system kinematic model (5) - (8)) are presented in Fig.9.
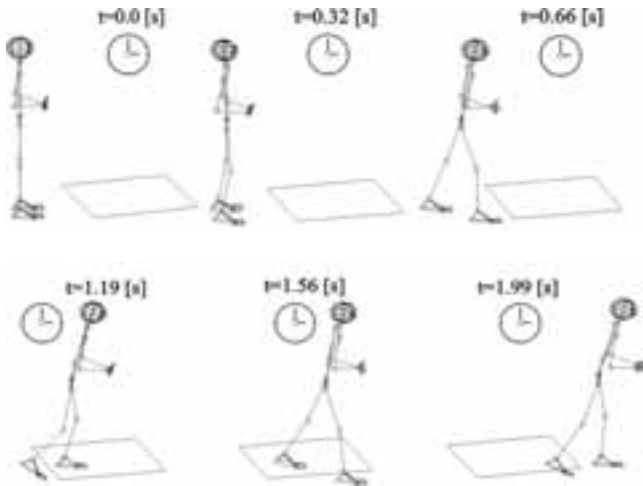
Figure 8. Snapshots of the computer simulation of the biped locomotion in several characteristic instants for the experimentally captured joint trajectories

Using relations (9), (24) and (25), the corresponding rates of change of functional coordinates were determined (Fig.10). They were used to define directly the impact model in the form of an LCP mathematical formulation.
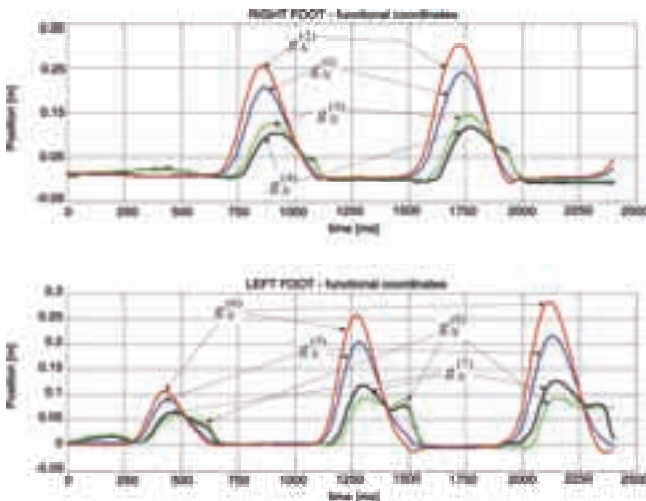
Figure 9. Functional coordinates $g_N^{(i)}$ determining the relative positions of the right and left feet contour points i=1,..,8 with respect to the support in the normal direction

The calculations based on the dynamic system model and models presented in Subsections 2.1 and 2.2 gave the ground reaction forces F_r^x, F_r^y, F_r^z for several half-steps illustrated in Fig.9.

The magnitudes of contact reaction forces in the directions normal to the ground and in the tangential (longitudinal and transversal) directions are given in Fig.11.

The encircled area DETAIL "A" shown in figure represents the time-history of change of the contact force F_r^z calculated on the basis of the model for the instants coincide with the instants when the real system (subject) was on the force-measuring platform (Fig.11, from $t = 1.19$ to $t = 1.56$ [s]). By analyzing the graphs presented in Fig.11, the following gait phases can be distinguished. At the beginning, the biped locomotion mechanism stands (rests) on both legs, whereby the contact forces on the left and right feet balance around the equilibrium value, equal to one half of the system weight, $G \cong 412$ [N]. After that, the biped starts to move, whereby the swing phase and the contact phase (the foot on the ground) are realized alternately. In the upper graph of Fig.11 it is possible to observe clearly the periodicity of steps succession that results in the change of contact force from zero value to the jerk, amplitude variation in the form of an M-function, and force vanishing. At the same time, the tangential forces too, exhibit their periodic character and dependence of the normal force of the foot pressure on the ground. Because of the presence of the wooden plates on the feet, whose coefficient of dry Coulomb's friction is approximately $\mu \approx 0.1$, the amplitudes of longitudinal and transversal forces are relatively small, $\left|F_r^x\right|, \left|F_r^y\right| \leq 100$ [N].

The accuracy of the considered model depends greatly on the identification accuracy of kinematic and dynamic parameters of the system. Under assumption that the precision of the laboratory measurements of movements was high and the trajectories of the biped joints were well-identified, the experimental results and results of simulation of the model dynamics should coincide or deviate minimally.

In Fig.12 the contact forces obtained by direct measurement on the platform and by model simulation are compared. As it can be seen, simulation results show the expected similarity to the experimental ones in respect of the shape of the function. Certain deviations of the amplitude magnitude (in the form of time lag) are a consequence of the presence of numerical noise in signal processing as well as of the application of the numeric filter which introduces certain time lagging.

In the control applications with the biped locomotion mechanisms using the dynamical model special attention should be paid to the quality of processing of the signals obtained by experimental measurements. A precise model identification is very important task. Also, high-quality filtering of numerical noise is needed.
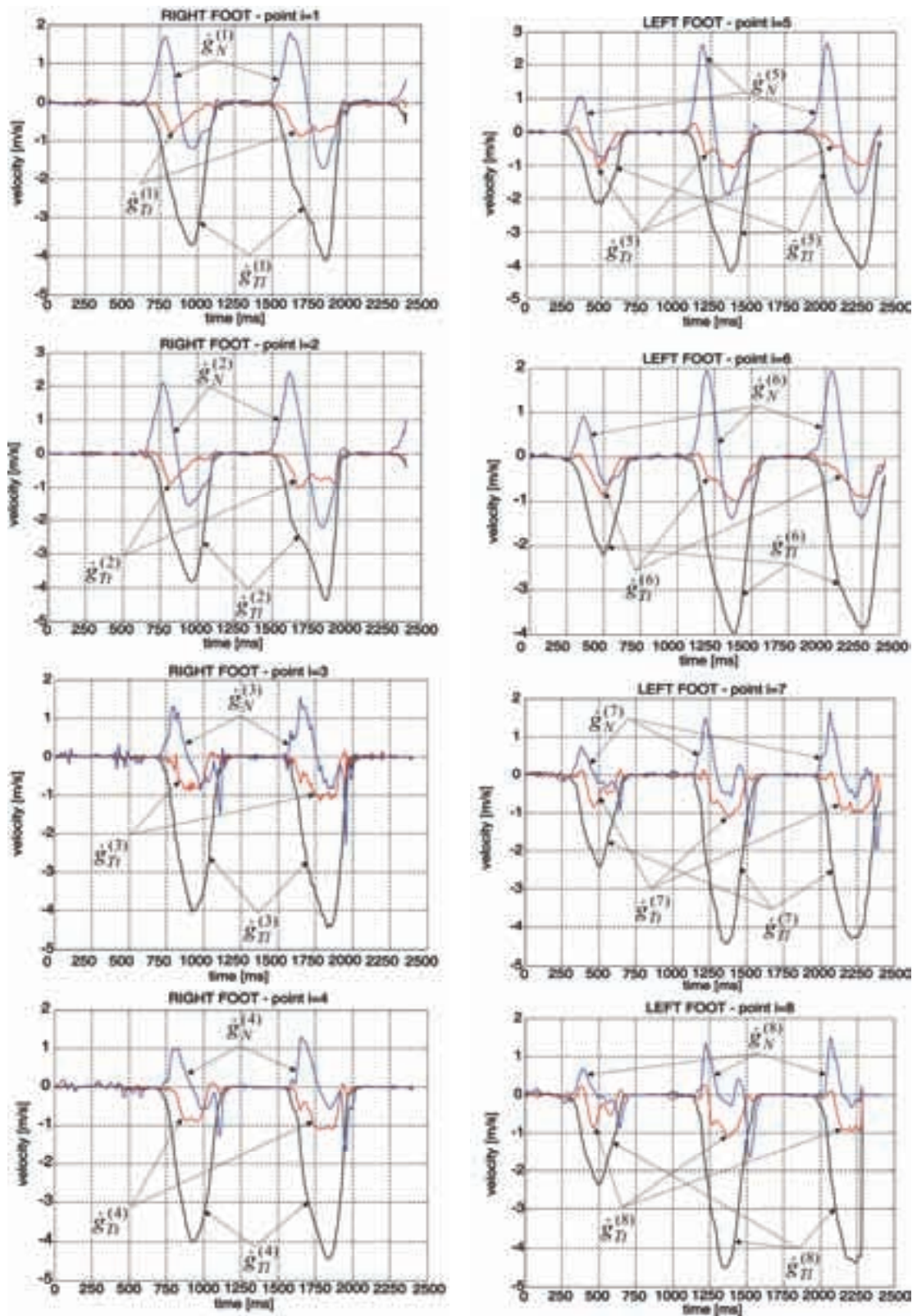
Figure 10. Derivatives of the functional coordinates (velocities) in the normal and tangential (longitudinal and transversal) directions of the feet displacements according to the point designations assumed in Fig.3
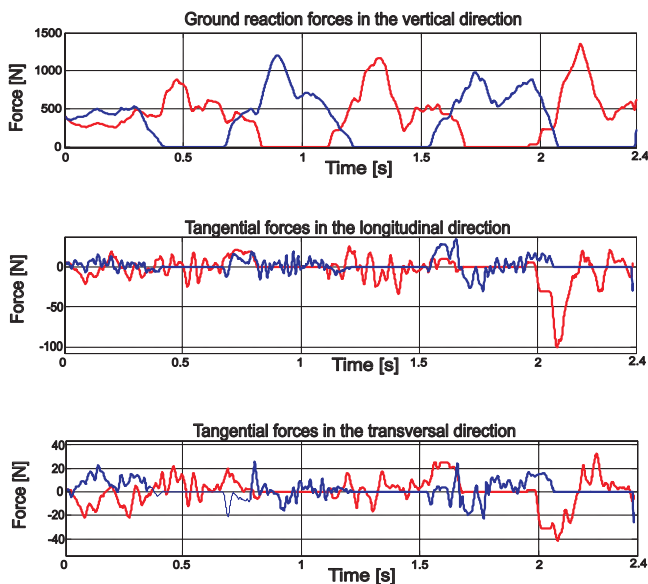
Figure 11. Model-based ground reaction forces at the right and the left foot during locomotion
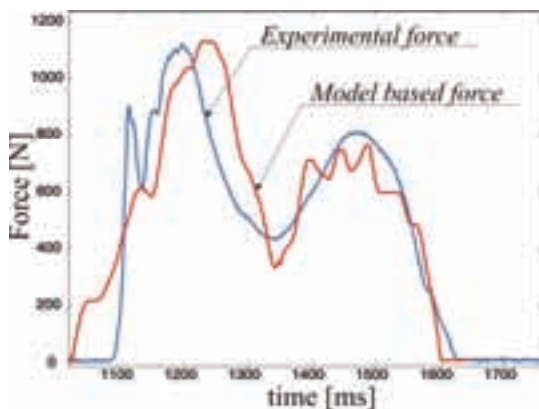
Figure 12. Comparison of the experimentally measured ground reaction force and the model-based force in the direction normal to the support

Summary

The work presents a general approach to modeling of biped locomotion systems. A special attention is paid to modeling impact dynamics and regular contact of the foot and the ground. The mechanical impact is of essential importance in various locomotion activities such as free walk, climbing/descending the staircase, jumping, etc. The problem of impact modeling is solved using the LCP mathematical formulation, known in the theory of rigid body mechanics. The validity of the derived model is tested by comparison with the experimental measurements on a human subject under laboratory conditions. Some characteristic results of experimental measurements of human gait are presented. The corresponding measurements served as the basis for determining joint trajectories of a hypothetic locomotion mechanism of anthropomorphic structure and parameters. The results of simulation of the biped system model are compared with the experimental ones. Similarity of the simulation and experimental results confirms the validity of the derived model of the biped system considered in contact with the support as a geometrical constraint. The results of the research performed in the paper are necessary for building human egzoskeletons potentially to be implemented with military tasks for increasing man-power capabilities.

References

[1] LIM,H.O., TAKANISHI,A.: *Compensatory motion control for a biped walking robot*, Robotica 23: pp.1-11, Part 1, (2005)

[2] VANDERBORGHT,B., VERRELST,B., VAN HAM,R., LEFEBER,D.: *Controlling a bipedal walking robot actuated by pleated pneumatic artificial muscles*, Robotica 24: Part 4, 2006, pp.401-410,

[3] YANG,C.X., WU,Q.: *On stabilization of bipedal robots during disturbed standing using the concept of Lyapunov exponents*, Robotica 24: Part 5, 2006, pp.621-624,

[4] VUKOBRATOVIĆ,M., BOROVAC,B., POTKONJAK,V., *Towards a unified understanding of basic notions and terms in humanoid robotics*, Robotica 25: Part 1, 2007, pp.87-101,

[5] Sarcos exoskeleton, available on line at: www.engadget.com/2007/11/25/sarcos-military-exoskeleton-becomes-a-frightening-reality/

[6] POTKONJAK,V., VUKOBRATOVIĆ,M.: *A Generalized Approach to Modeling Dynamics of Human and Humanoid Motion*, International Journal of Humanoid Robotics, World Scientific Publishing Company, 2, 2005, No.1, pp.21-45.

[7] VUKOBRATOVIĆ,M., RODIC,A.: *Contribution to the Integrated Control of Biped Locomotion Mechanisms*, International Journal of Humanoid Robotics, World Scientific Publishing Company, March 2007, Vol.4, No.1, pp.49-95.

[8] BOYER,K.A., NIGG,B.M.: *Muscle activity in the leg is tuned in response to impact force characteristics*, Jour. Biomech. 37(10): 2004, pp.1583-1588.

[9] GERRITSEN,K.G., VAN DEN BOGERT,A.J., NIGG,B.M.: *Direct dynamics simulation of the impact phase in heel-toe running*, Jour. Biomech. 28(6): 1995, pp.661-668.

[10] NURSE,M.A., HULLIGER,M., WAKELING,J.M., NIGG,B.M.: Stefanyshyn D. J., *Changing the texture of footwear can alter gait patterns*, Jour. Electromyogr. Kinesiol 15(5): 2005, pp.496-506.

[11] NURSE,M.A., NIGG,B.M.: *Quantifying a relationship between tactile and vibration sensitivity of the human foot with plantar pressure distributions during gait*, Clin. Biomech. (Bristol, Avon) 14(9): 1999, pp.667-672.

[12] PFEIFER,F. GLOCKER,Ch.: *Multibody Dynamics with Unilateral Contacts*, John Willey \& Sons, Inc., 1996.

[13] BROGLIATO,B.: *Nonlinear Impact Mechanics: Models, Dynamics and Control*, Springer-Verlag, London, 1996.

[14] VUKOBRATOVIĆ,M., BOROVAC,B., SURLA,D., STOKIC,D.: *Biped Locomotion: Dynamics, Stability, Control and Application*, Springer-Verlag, 1989.

[15] PARK,J., CORTESAO,R., KHATIB,O.: *Multi-contact compliant motion control for robotic manipulators*, 2004 IEEE International Conference on Robotics and Automation, Proceedings ICRA04, 2004, Vol.5, pp.4789 – 4794.

[16] KHATIB,O., SENTIS,L., PARK,J., WARREN,J.: *Whole-body dynamic behavior and control of human-like robots*, Int. Jour. of Humanoid Robotics, 1(1): 2004, pp.29-43.

[17] Stewart,D.: *A Platform with Six Degrees of Freedom*, The Institution of Mechanical Engineers, Proceedings 1965-66, 180 Part 1, No.15, pp.371-386.

[18] VUKOBRATOVIĆ,M., POTKONJAK,V., RODIĆ,A.: *Contribution to the Dynamic Study of Humanoid Robots Interacting with Dynamic Environment*, International Journal Robotica, 22, 2004, pp.439-447.

[19] LEMKE,C.A.: *Some pivot scheme for the linear complementarity problem*, In: Balinsky ML, Cottle RW (eds): Mathematical programming studies, 1978, Vol.7, pp.15-35.

[20] ZATSIORSKY,V., SELUYANOV,V., CHUGUNOVA,L.: *Methods of Determining mass-inertial Characteristics of Human Body Segments*, Contemporary Problems of Biomechanics, 1990, pp.272-291, CRC Press.

[21] De LEVA,P.: *Adjustments to Zatsiorsky-Seluyanov's segment Inertia Parameters*, Journal of Biomechanics, Vol.29, No.9, pp.1223-1230, (1996).

[22] Matlab/Simulink engineering toolbox, 6.5, R13, Mathworks, 2004

[23] PAUL,R.P.: *Robot Manipulators: Mathematics, Programming, and Control*, The MIT Press, Cambridge, Massachustets \& London, England, 1981.

[24] CORKE,P.I.: *Robotics Toolbox for Matlab*, Release 6, CSIRO, Manufacturing Science and Technology, Pinjara Hills, Australia, (2001). http://www.cat.csiro.au/cmst/staff/pic/robot 447453

Modeliranje fenomena udara kod dvonožnih lokomocionih mehanizama – Teorija i Eksperimenti

U radu se predlaže jedan opšti pristup matematičkom modeliranju dvonožnih lokomocionih sistema (čoveka i čovekolikih robota) s specijalnom pažnjom posvećenom udarnoj i kontaktnoj dinamici. Modeliranje udarne dinamike kod različitih lokomocionih mehanizama ima značajnu ulogu u robotici kao i vojnim primenama zbog neophodnosti adaptacije mehanizama na nepoznate i nestrukturane terene. Umesto uobičajenog induktivnog pristupa, koji počinje od analize različitih situacija realnog kretanja (hoda, trčanja, skokova, penjanja na prepreke, podizanja tereta, isl.) i pokušava da pravi generalizaciju problema, u ovom radu se bavimo jednim deduktivnim pristupom rešavanju kod koga je razmatran celovit problem pa su onda razmatrane specifičnosti. Dinamika udara je modelirana primenom tzv. Linear Complementarity Problem (LCP) formulacije. Demonstrirana je i objašnjena jedna opšta metodologija primenjiva kod humanoidnih robota na bazi sinteze prostornog modela dvonožnog sistema. Valjanost jednog ovakvog pristupa modeliranju je potvrđena eksperimentalnim merenjima na ljudima u laboratorijskim uslovima. U radu su prikazani grafički prikazi koji ilustruju eksperimentalne rezultate merenja kao i rezultate odgovarajućih simulacionih testova.

Ključne reči: robotika, lokomotorni sistem, modelovanje sistema, matematičko modelovanje, kontaktna dinamika, kontaktno opterećenje, udarno opterećenje.

Моделирование феномена удара у двуногих локомоционных механизмов - Теория и эксперименты

В настоящей работе предлагается один общий подход к математическому моделированию двуногих локомоционных систем (человека и интеллектуального робота) со специальным вниманием, посвящённым ударной и контактной динамике. Моделирование ударной динамики у различных локомоционных механизмов имеет значительную роль в робототехнике, а в том числе и в военных применениях, ради необходимости приспособления механизмов к неизвестным и неструктурным местностям. Вместо привычного индукционного подхода, начинающего с анализа различных ситуаций реального движения (хода, бега, прыжков, поднимания на препятствия, поднимания груза... и.т.п.) и попытающего сделать обобщение проблем, в настоящей работе представлен дедукционный подход к разрешению с рассматриванием целостной проблемы, а потом отдельных специфичностей. Динамика удара моделирована применением так называемой Линеар Цомплементеритю Проблем (ЛЦП) формулировкой. Здесь показана и растолкована одна общая методология применима у интеллектуальных роботов на основании синтеза объёмной модели двуногой системы. Справедливость одного такого подхода к моделированию обоснованна и доказана экспериментальными измерениями на людях в лаборатных условиях. В работе представлены графики, иллюстрирующие экспериментальные результаты измерений, а в том числе и результаты соответствующих имитирующих испытаний.

Ключевые слова: робототехника, локодвигательная система, моделирование системы, математическое моделирование, контактная динамика, контактная нагрузка, ударная нагрузка.

Modélisation des phénomènes d'impact pour les mécanismes de locomotion bipède -Théorie et Expériences

Cet article suggère une approche généralisée à la modélisation mathématique des systèmes ayant une locomotion bipède (humains ou robots humanoïdes) avec une attention particulière portée à l'impact et à la dynamique du contact. La modélisation de la dynamique de l'impact pour des mécanismes divers de locomotion présente un intérêt significatif en robotique et pour les applications militaires en raison de l'adaptation nécessaire des mécanismes à l'incertitude des terrains accidentés. Au lieu de l'approche *inductive* qui débute par une analyse de différentes situations rencontrées dans le mouvement réel (marche à pied, course, bond, franchissement d'obstacles, transport de charges, etc…) et qui tente ensuite d'en faire une généralisation, une approche déductive est proposée, où le problème général est considéré. La dynamique de l'impact est modélisée sous forme d'un problème de complémentarité linéaire (LCP). La méthodologie générale est expliquée et démontrée avec un robot humanoïde via la synthèse d'un modèle bipède. La validité de l'approche de modélisation est confirmée par des mesures expérimentales sur un sujet humain dans les conditions de laboratoire. De nombreuses présentations graphiques illustrant les résultats expérimentaux aussi bien que les résultats des simulations correspondantes, sont présentées.

Mots clés: robotique, système locomoteur, modélisation du système, modélisation mathématique, dynamique du contact, charge de contact, charge d'impact.